

Supplementary data for

A click mediated route to a novel fluorescent pyridino-extended calix[4]pyrrole sensor: synthesis and binding studies

Ahmad Rifai^b, Nancy AlHaddad^{a,b}, Manale Noun^b, Ismail Abbas^c, Malek Tabbal^d, Rania Shatila^d, Francine Cazier-Dennin^a and Pierre-Edouard Danjou^{*a}

^aUnité de Chimie Environnementale et Interactions sur le Vivant (UCEIV) - Université du Littoral Côte d'Opale, 145 Avenue Maurice Schumann, MREI 1, 59140 Dunkerque, France. E-mail : danjou@univ-littoral.fr

^bLebanese Atomic Energy Commission – National Council for Scientific Research – B. P. 11- 8281, Riad El Solh 1107 2260 Beirut - Lebanon

^cDepartment of Chemistry -Faculty of Sciences 1 – Lebanese University – Hadath – Lebanon.

^dDepartment of Physics - American University of Beirut - Riad el Solh, Bliss St. - P.O. Box; 11-0236 - 1107 2020 – Beirut - Lebanon

Figure 1: ¹ H NMR spectrum (400MHz, 298K) of CP2 in CDCl ₃	1
Figure 2: ¹³ C NMR spectrum (101 MHz, 298K) of CP2 in CDCl ₃	1
Figure 3: COSY NMR spectrum (400MHz, 298K) of CP2 in CDCl ₃	2
Figure 4: HSQC NMR spectrum (400MHz, 298K) of CP2 in CDCl ₃	2
Figure 5: ¹ H NMR spectrum (500MHz, 298K) of CP3 in d ₆ -DMSO.....	3
Figure 6: ¹³ C NMR spectrum (125 MHz, 298K) of CP3 in d ₆ -DMSO.....	3
Figure 7: COSY NMR spectrum (500MHz, 298K) of CP3 in d ₆ -DMSO.....	4
Figure 8: HSQC NMR spectrum (500MHz, 298K) of CP3 in d ₆ -DMSO.....	4
Figure 9 : Excitation and emission spectra of CP3 (λ _{ex} = 300 nm, λ _{em} = 446 nm) in DMSO.....	5
Figure 10 : Fluorescence Decay of CP3 in DMSO (NanoLED source light of 330 nm, channel width = 82 ns, 0.0274348ns/channel).....	5
Figure 11 : ¹ H NMR spectra for the titration of CP3 (a) in d ₆ -DMSO with TBACl (b), TBABr (c), TBAI (d), TBAHSO ₄ (e) and TBAF (f).....	6
Figure 12 : Change in fluorescence emission of CP3 (5*10 ⁻⁵ M, λ _{ex} = 300 nm, DMSO) upon addition of 10 equivalents of TBAF, TBACl, TBABr, TBAI and TBAHSO ₄	6
Figure 13 : Job plot of CP3.F ⁻ complex.....	7
Figure 14: Fluorescence quenching of CP3 with Fe(ClO ₄) ₃ and calculated curve for A) 1:1 complex and B) mix of 1:1 and 1:2 complexes.....	9
Figure 15: Fluorescence quenching of CP3 with Fe(ClO ₄) ₂ and calculated curve for 1:1 complex.....	9

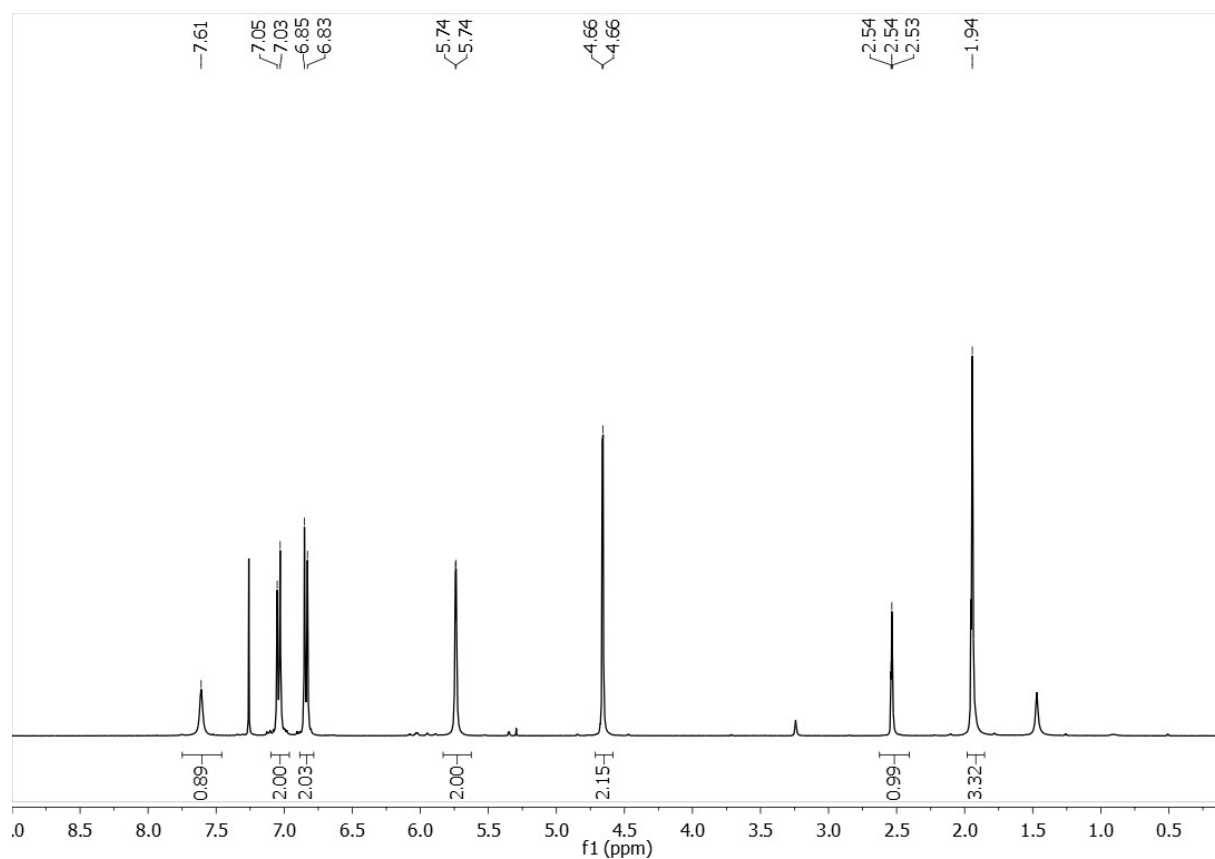


Figure 1: ¹H NMR spectrum (400MHz, 298K) of CP2 in CDCl₃.

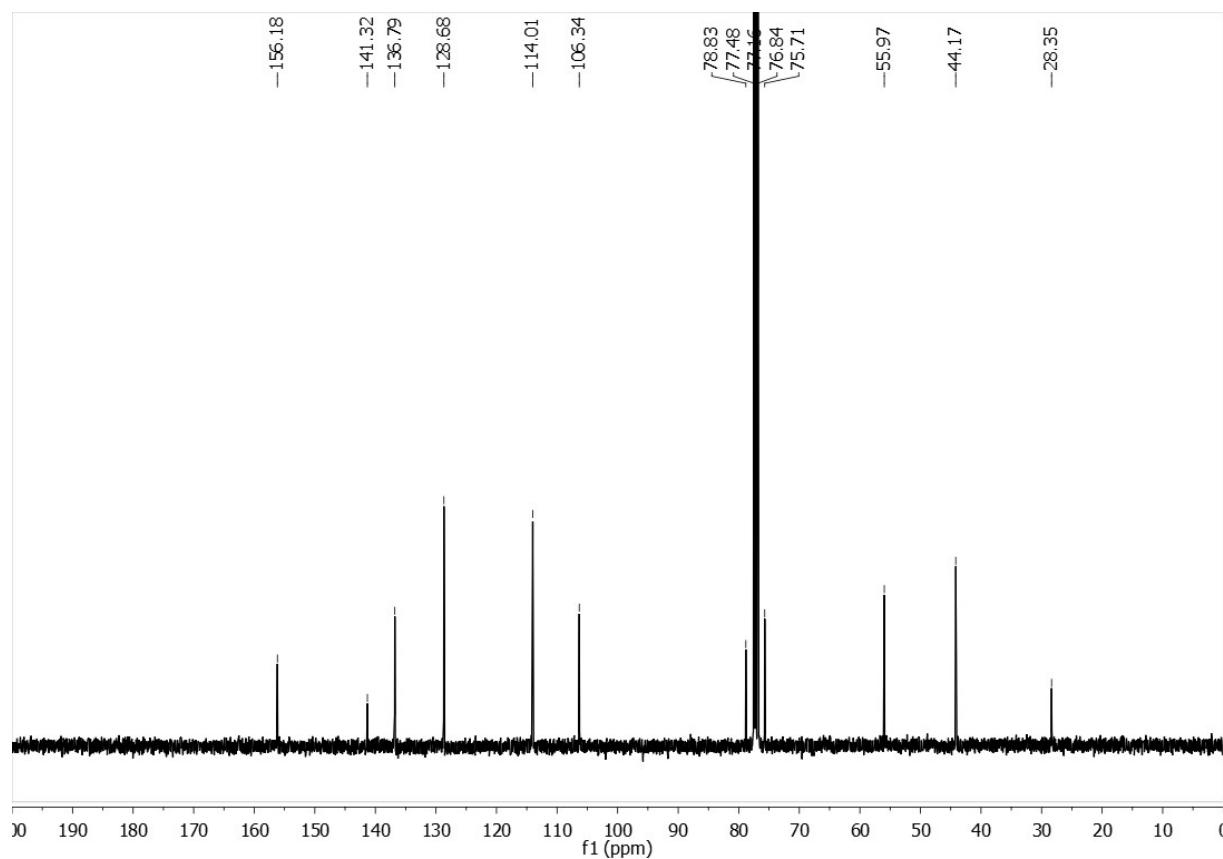


Figure 2: ¹³C NMR spectrum (101 MHz, 298K) of CP2 in CDCl₃.

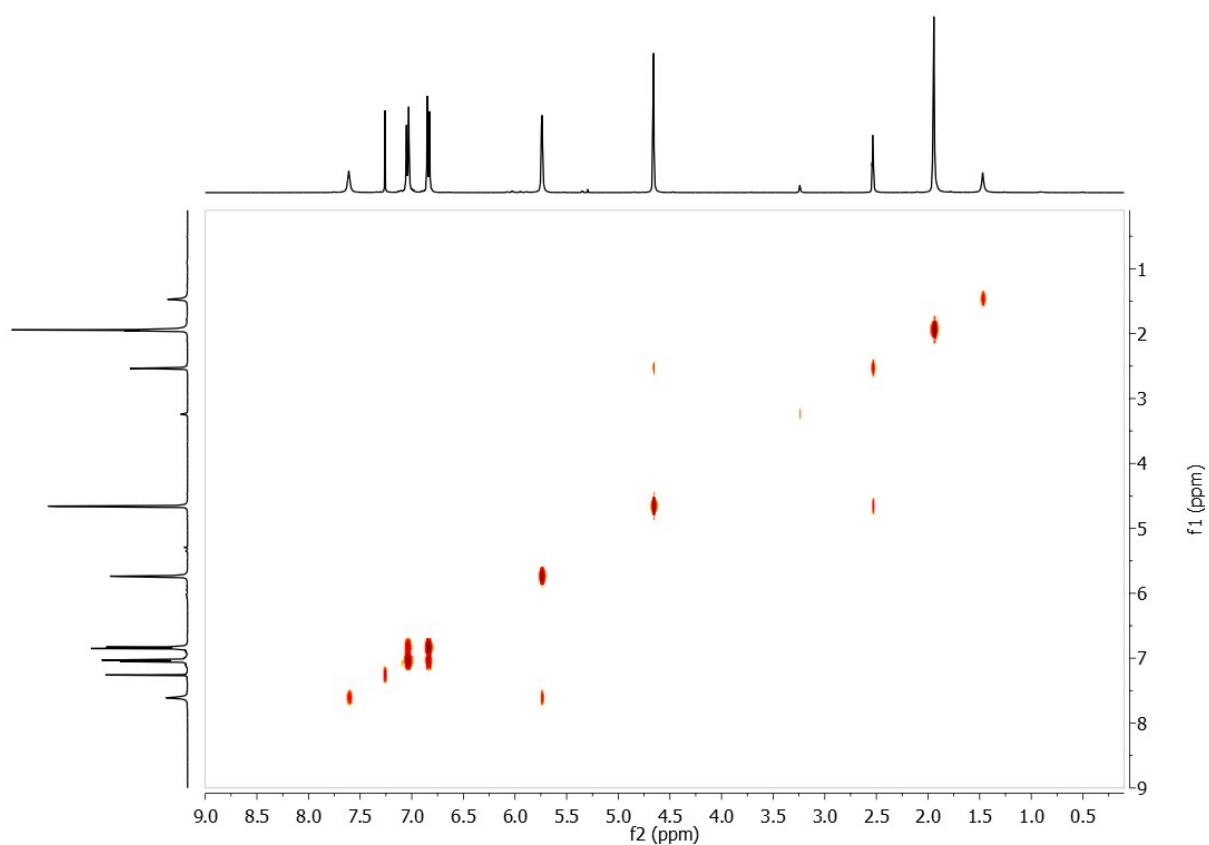


Figure 3: COSY NMR spectrum (400MHz, 298K) of CP2 in CDCl₃.

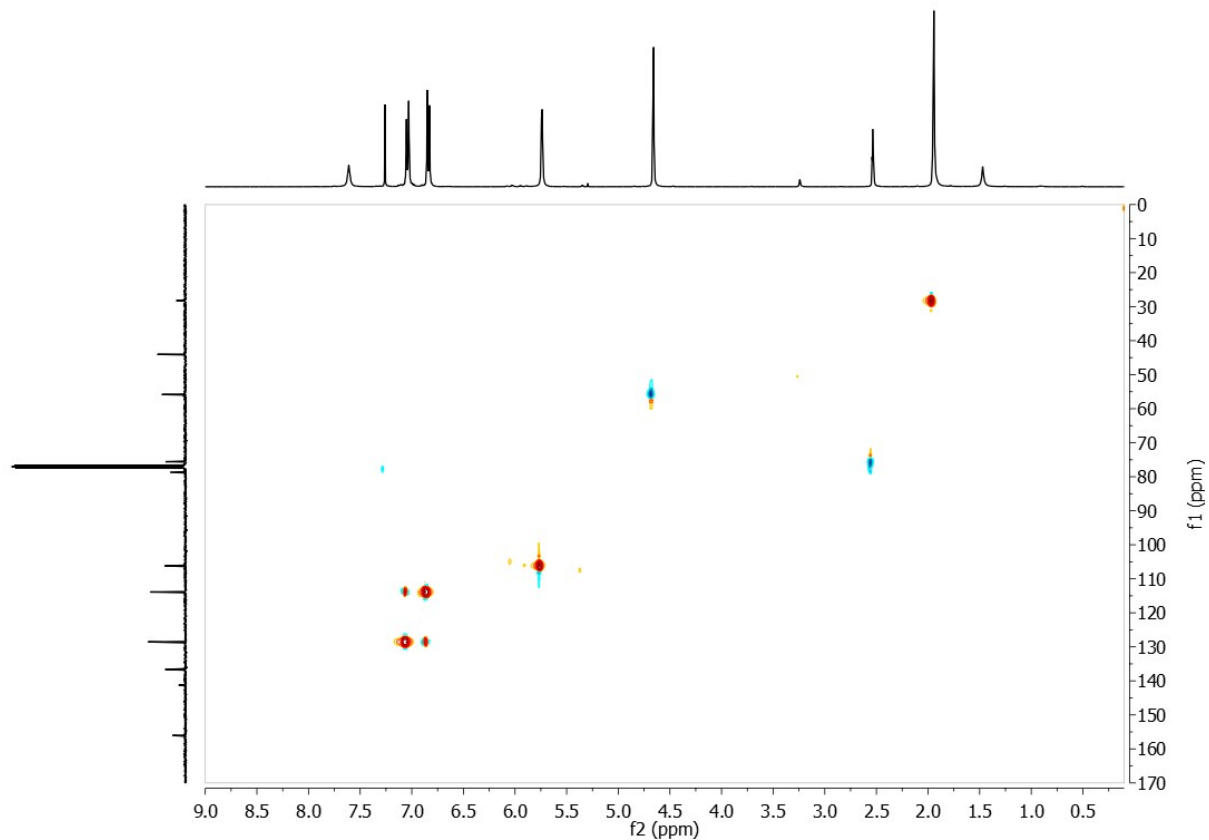


Figure 4: HSQC NMR spectrum (400MHz, 298K) of CP2 in CDCl₃

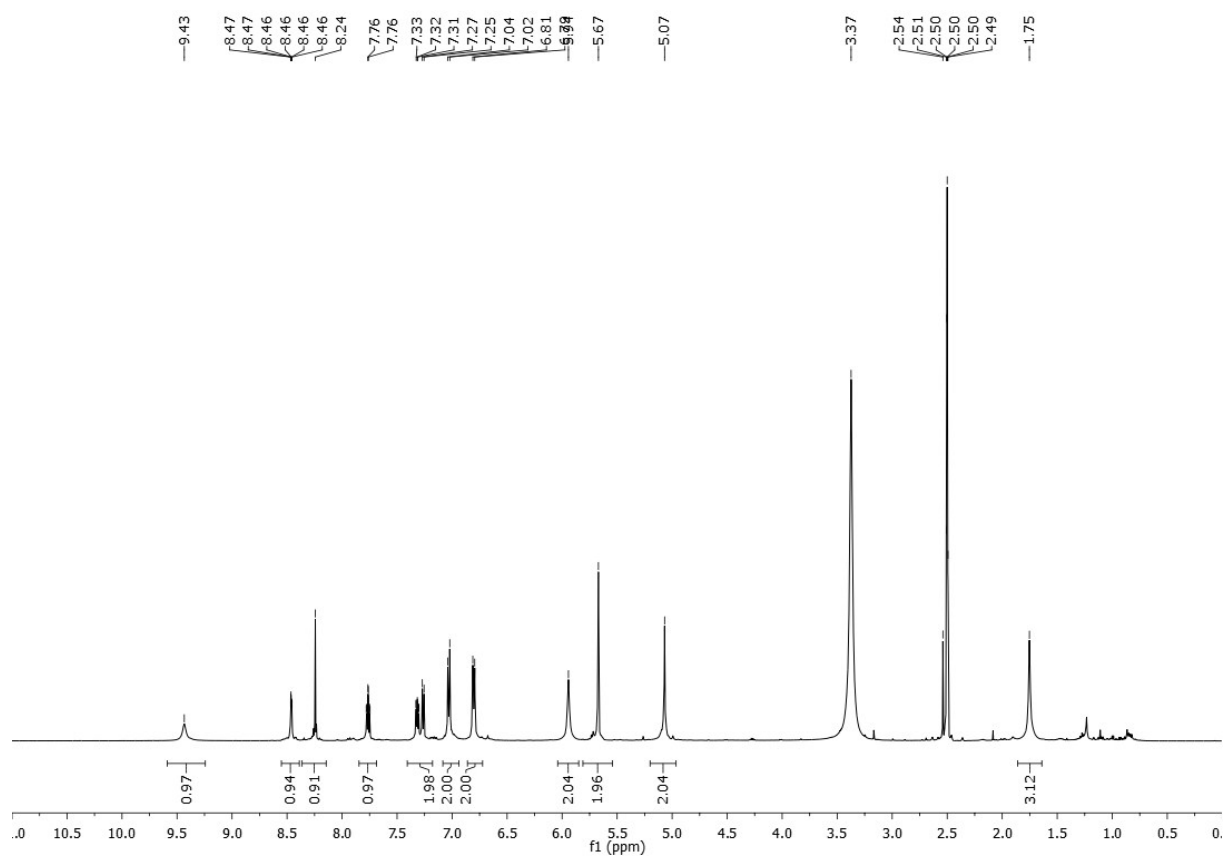


Figure 5: ¹H NMR spectrum (500 MHz, 298 K) of CP3 in d₆-DMSO.

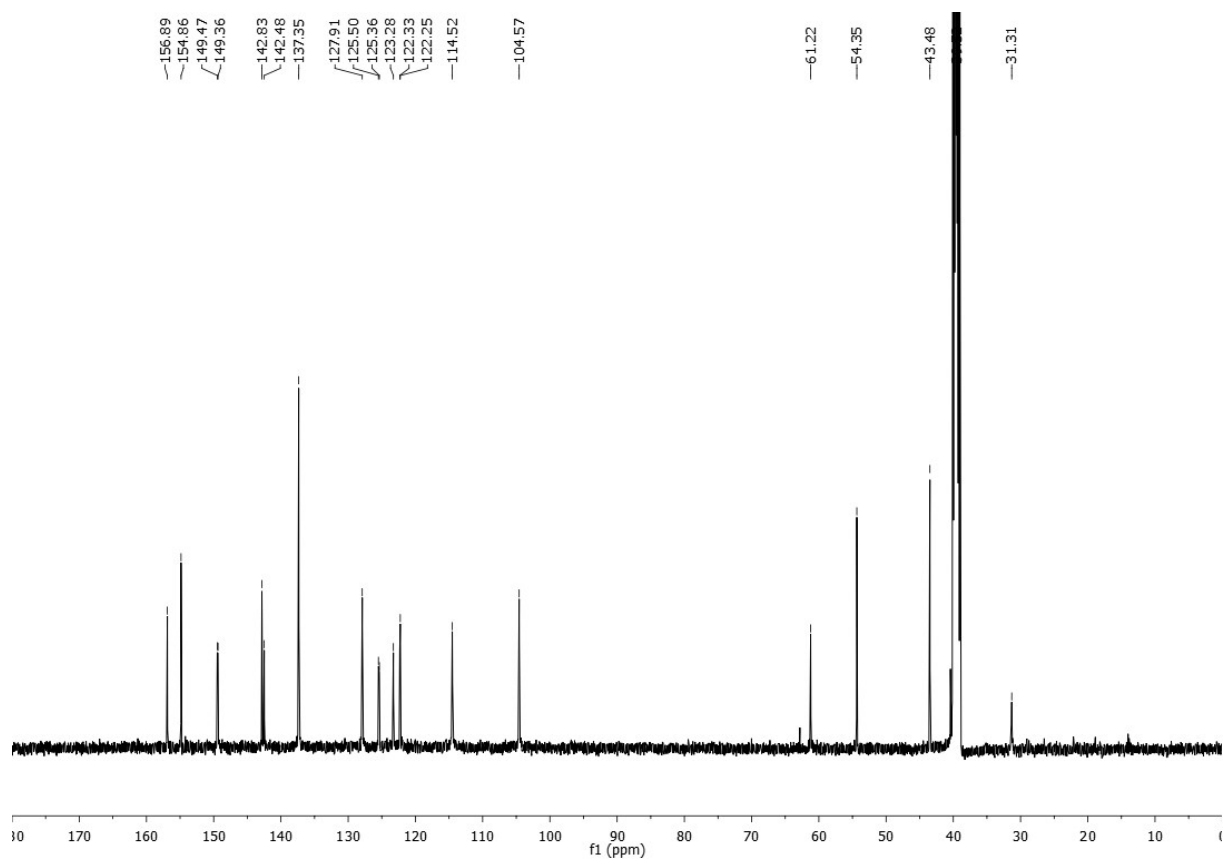


Figure 6: ¹³C NMR spectrum (125 MHz, 298 K) of CP3 in d₆-DMSO.

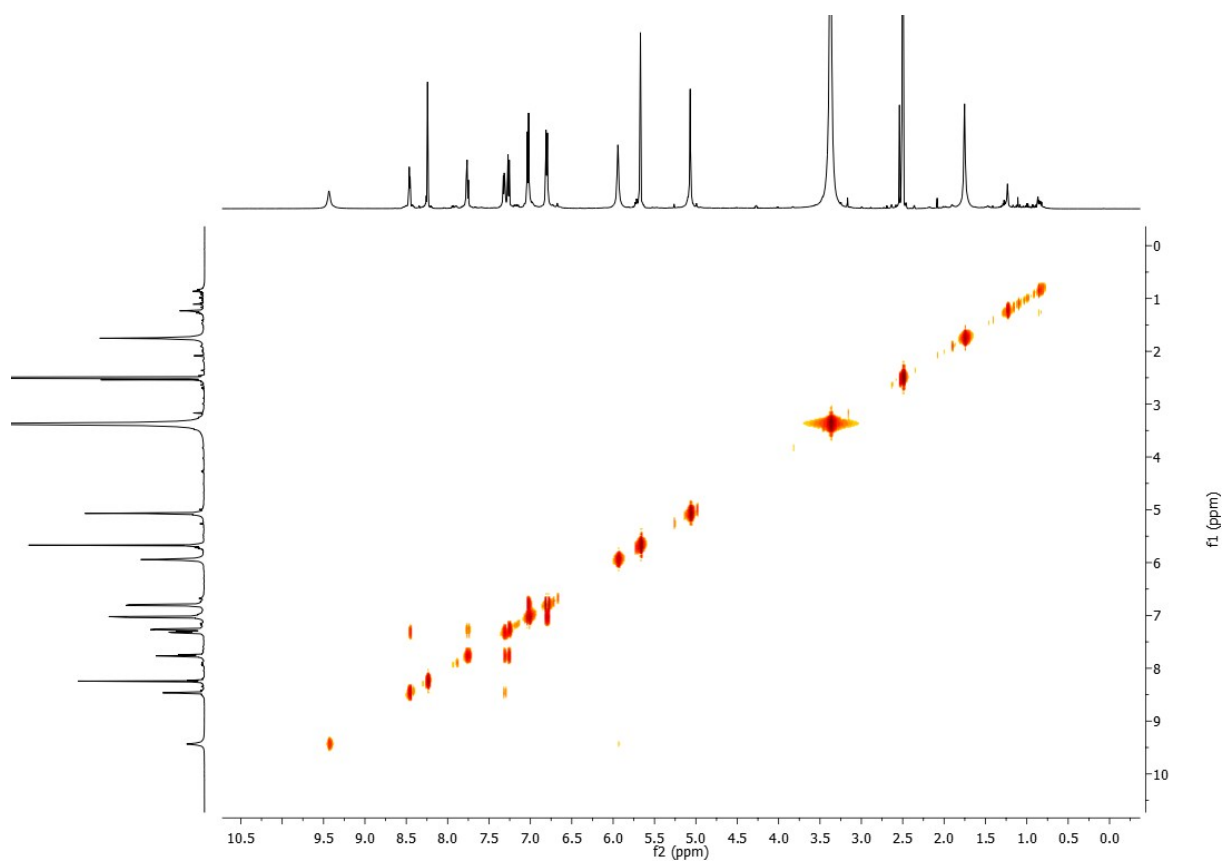


Figure 7: COSY NMR spectrum (500MHz, 298K) of CP3 in d6-DMSO.

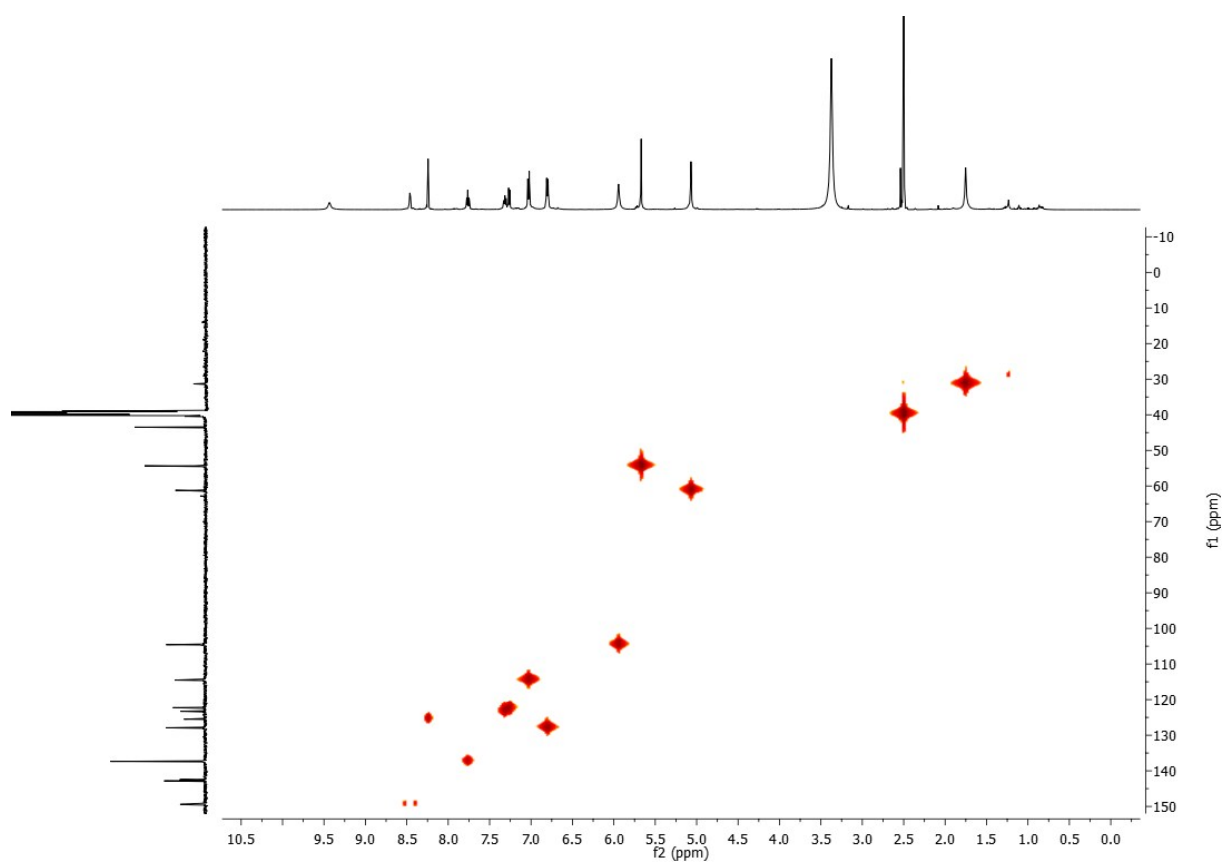


Figure 8: HSQC NMR spectrum (500MHz, 298K) of CP3 in d6-DMSO.

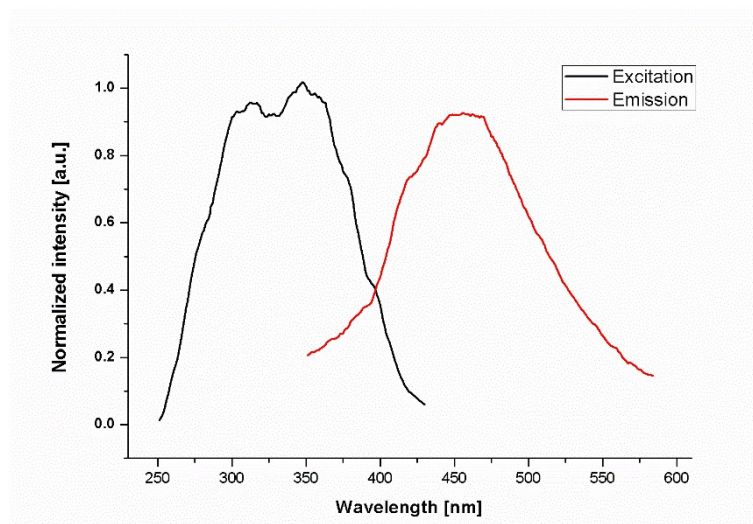


Figure 9 : Excitation and emission spectra of CP3 ($\lambda_{\text{ex}} = 300 \text{ nm}$, $\lambda_{\text{em}} = 446 \text{ nm}$) in DMSO

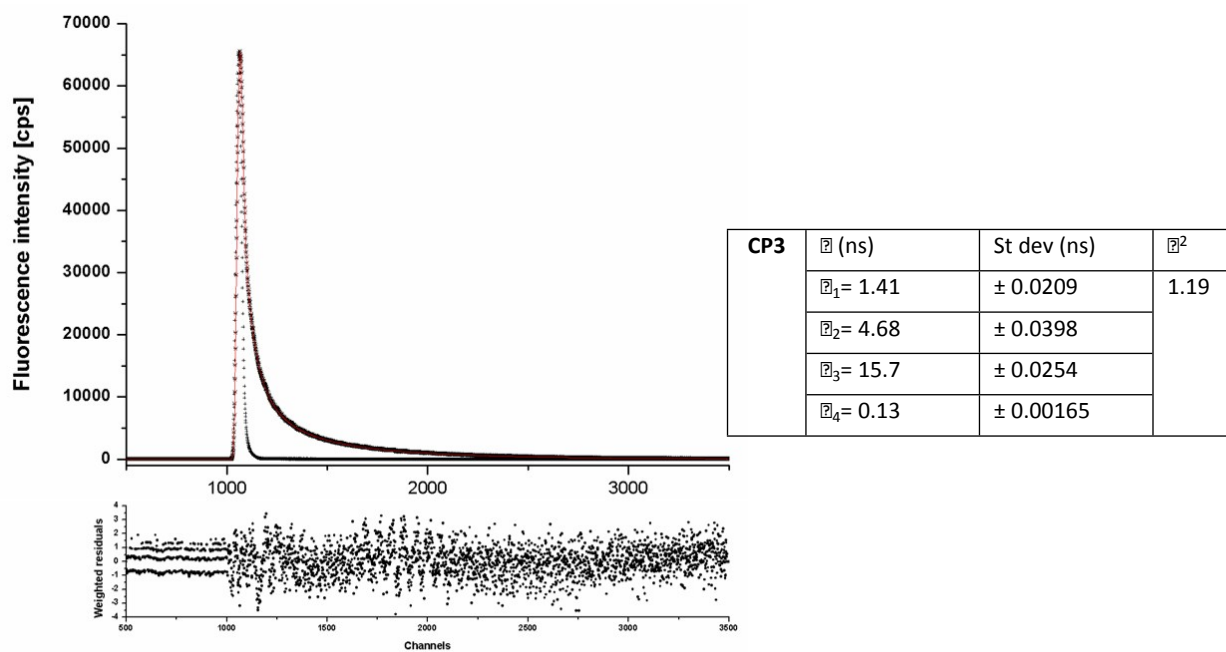


Figure 10 : Fluorescence Decay of CP3 in DMSO (NanoLED source light of 330 nm, channel width = 82 ns, 0.0274348ns/channel)

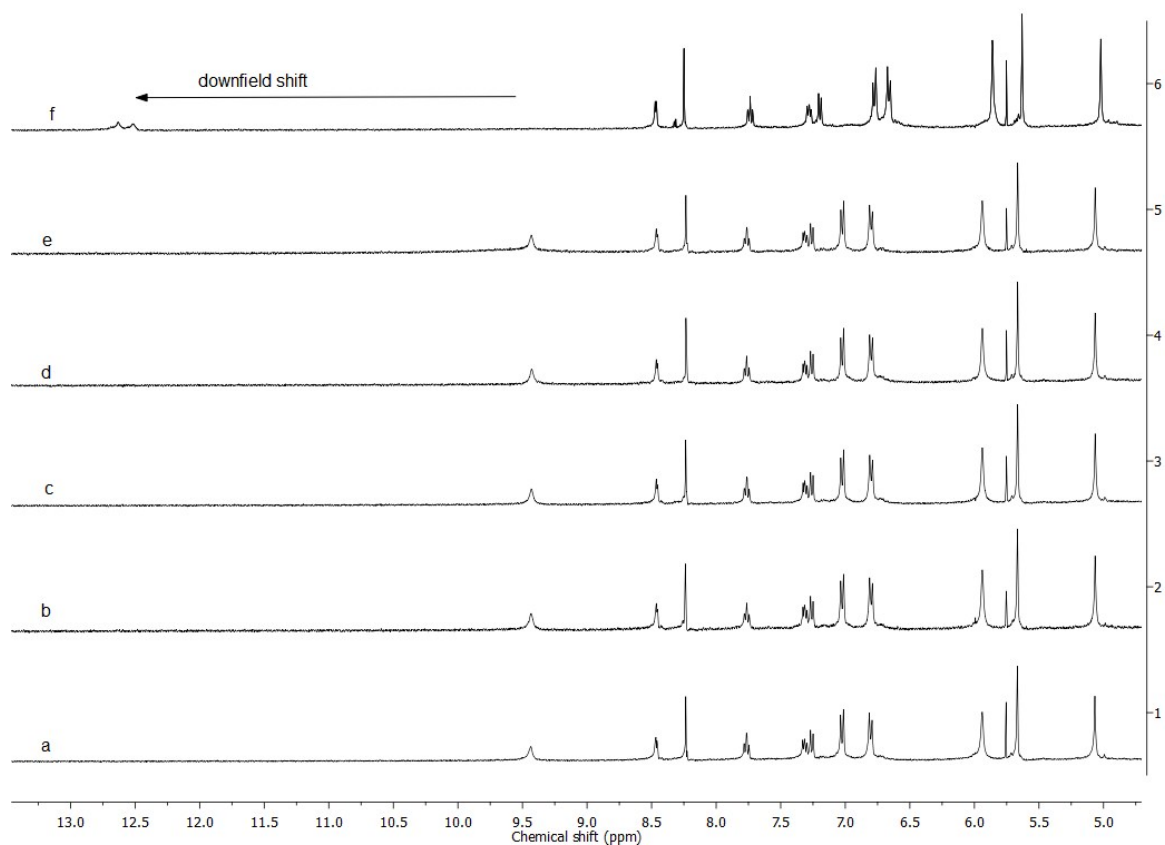


Figure 11 : ^1H NMR spectra for the titration of CP3 (a) in d_6 -DMSO with TBACl (b), TBABr (c), TBAI (d), TBAHSO₄ (e) and TBAF (f).

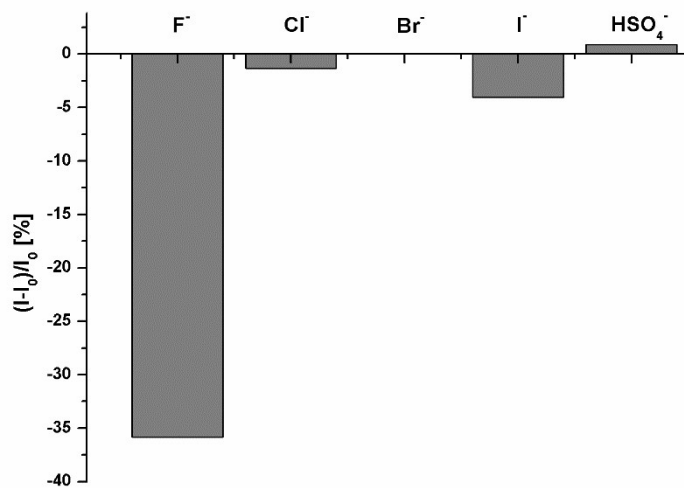


Figure 12 : Change in fluorescence emission of CP3 ($5 \times 10^{-5}\text{M}$, $\lambda_{\text{ex}} = 300\text{ nm}$, DMSO) upon addition of 10 equivalents of TBAF, TBACl, TBABr, TBAI and TBAHSO₄.

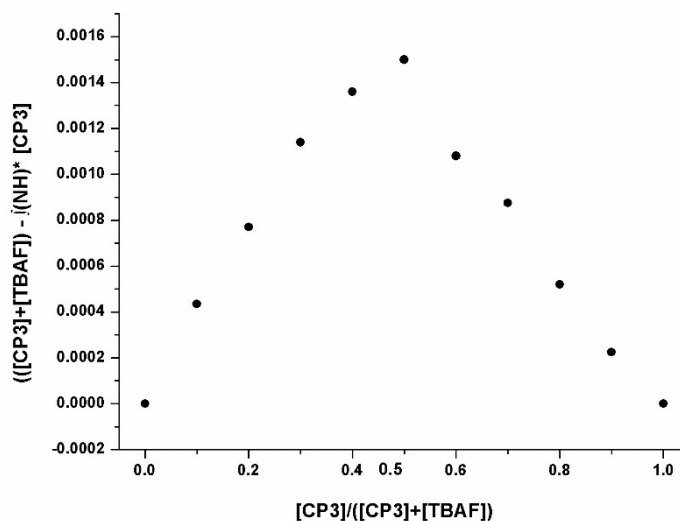


Figure 13 : Job plot of CP3.F⁻ complex.

Fluorescence data treatment [1]

Fluorescence data were treated with a general equilibrium model (developed in our team and implemented within Excel), even if, in this work, only 1:1, 1:1+2:1 and 1:1+1:2 stoichiometric combinations were investigated. In the general model, we consider a single host (H) which may potentially interact with a first guest (A) under 1:1 and 2:1 stoichiometry, and/or a second guest (B) under 1:1 and 1:2 stoichiometry. Accordingly, the following equations describe the corresponding equilibriums:



$$K_{H-A} = \frac{[H - A]}{[H] * [A]} \quad (2)$$



$$K_{H-B} = \frac{[H - B]}{[H] * [B]} \quad (4)$$



$$K_{H_2-A} = \frac{[H_2 - A]}{[H - A] * [H]} \quad (6)$$



$$K_{H-B_2} = \frac{[H-B_2]}{[H-B] * [B]} \quad (8)$$

$$[A]_T = [A] + [H-A] + [H_2-A] \quad (9)$$

$$[B]_T = [B] + [H-B] + 2 * [H-B_2] \quad (10)$$

$$[H]_T = [H] + [H-A] + 2 * [H_2-A] + [H-B] + [H-B_2] \quad (11)$$

$[A]_T$ may be defined as a function of $[H]$, by combining equations (9) with (2) and (6):

$$[A]_T = [A] * \left[1 + K_{H-A} * [H] + K_{H_2-A} * K_{H-A} * [H]^2 \right] \quad (12)$$

which leads to:

$$[A] = \frac{[A]_T}{\left[1 + K_{H-A} * [H] + K_{H_2-A} * K_{H-A} * [H]^2 \right]} \quad (13)$$

$[B]_T$ may also be defined as a function of $[H]$, by combining equations (10) with (4) and (8):

$$[B]_T = [B] + K_{H-B} * [H] * [B] + 2 * K_{H-B_2} * K_{H-B} * [H] * [B]^2 \quad (14)$$

The physical root of this quadratic polynomial is then defined by equation (15):

$$[B] = \sqrt{\frac{[B]_T}{2 * K_{H-B_2} * K_{H-B} * [H]} + \left[\frac{(1 + K_{H-B} * [H])}{4 * K_{H-B_2} * K_{H-B} * [H]} \right]^2} - \frac{(1 + K_{H-B} * [H])}{4 * K_{H-B_2} * K_{H-B} * [H]} \quad (15)$$

Defining $[H]_T$ as a function of $[H]$ leads to equation (16)

$$\begin{aligned} [H]_T &= [H] + K_{H-A} * [H] * [A] + 2 * K_{H_2-A} * K_{H-A} * [H]^2 * [A] + K_{H-B} * [H] * [B] + K_{H-B_2} * [H] * [B]^2 \end{aligned} \quad (16)$$

As $[A]$ and $[B]$ are complex functions of $[H]$, equation (16) corresponds to a binding polynomial of degree 4. As a consequence, there is no analytical form for the corresponding physical root, which has to be obtained by a numerical approach (Newton's method). Finally, $[H-A]$, $[H-B]$, $[H_2-A]$, and $[H-B_2]$ equilibrium concentrations can be calculated by the use of equations (2), (4), (6) and (8), respectively.

Accordingly, all combinations of equilibria described by equation (1), (3), (5) and (7) may be simulated by such treatment, by considering a significant or, to the contrary, negligible formation constant for each envisaged or non-envisaged complex. In this work, significant values of affinity were considered for 1:1 and/or 2:1 and/or 1:2 stoichiometries, thus leading to the evaluation of equation (1) alone, of the combination of equations (1) and (5) and of the combination of (3) and (7).

Then, fluorescence intensities (F) may be calculated on the basis of equation (17) :

$$F = F_H + F_{H-A} + F_{H-B} + F_{H_2-A} + F_{H-B_2} \quad (17)$$

With each hypothetical F_X molecular contribution to fluorescence (X referring to H, H-A, H-B, H_2 -A or H-B₂) being given by equation (18) :

$$F_X = f_X * [X] \quad (18)$$

f_X being the fluorescence response factor of a given species.

The root mean square deviations (RMSD) between experimental and theoretical data is finally minimized by Newton-Raphson method, by varying formation constants and fluorescence response factors. If a quenching phenomenon is expected, a fluorescence response factor close to zero should be obtained for each complex, at the end of the algorithmic treatment. Uncertainty on each estimated parameters are estimated by calculation of variance–covariance matrixes.

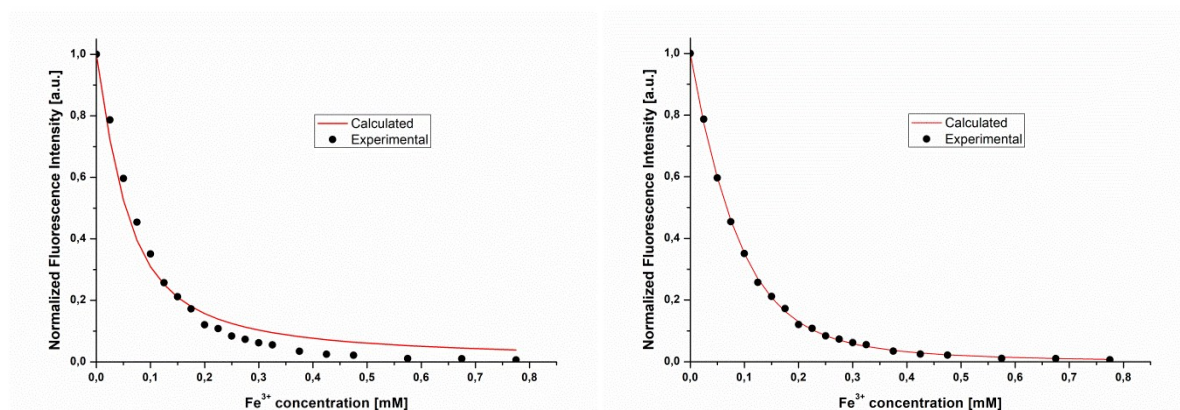


Figure 14: Fluorescence quenching of CP3 with $Fe(ClO_4)_3$ and calculated curve for A) 1:1 complex and B) mix of 1:1 and 1:2 complexes.

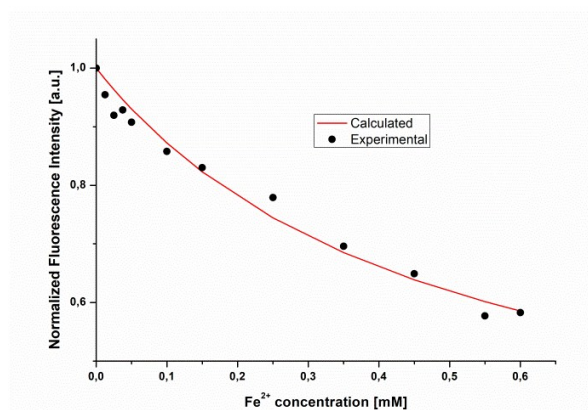


Figure 15: Fluorescence quenching of CP3 with $\text{Fe}(\text{ClO}_4)_2$ and calculated curve for 1:1 complex.

[1] Landy, D. "Measuring Binding Constants of Cyclodextrin Inclusion Compounds". In Cyclodextrin Fundamentals, Reactivity and Analysis. Springer International Publishing AG. S. Fourmentin et al. (eds.). Environmental Chemistry for a Sustainable World, 2018. ISBN 978-3-319-76159-6. DOI 10.1007/978-3-319-76159-6